AADE-08-DF-HO-27

Yield Stress: What is the "True" Value?

Jason Maxey, Baker Hughes Drilling Fluids; Randy Ewoldt, Peter Winter, and Gareth McKinley, Massachusetts Institute of Technology

Abstract

Great significance is placed on the yield stress that is determined for a drilling fluid. Less agreement is found on what an appropriate range of yield stress may be for a fluid system; nevertheless, most will agree that a sufficient yield stress is critical for maintaining suspension of cuttings and weight materials. However, the relevance of any particular yield stress value for any drilling fluid is questionable.

While some rely on the traditional Bingham plastic model and the yield point it predicts, this model and its method of application has been found to be lacking in accuracy when examining drilling fluids. The new API specification of the Herschel-Bulkley model for prediction of fluid parameters provides a yield stress that can be significantly different than predicted by the Bingham plastic model. But is this value any more indicative of the yield stress as directly measured by rheological methods? On top of this lies the question of what methodology is most appropriate for direct measurement of the yield stress?

In this paper, a series of water-based and invert emulsion fluids are studied through various methods. A comparison of the results of yield stress predictions and direct yield stress measurements will be made. Some effort is also given to determining which of these is best applied to the study and evaluation of drilling fluids.

Introduction

The performance of a drilling fluid is strained by the intermittent nature of drilling. While drilling ahead, relatively long periods of fluid flow will be interrupted by short periods (usually less than ten minutes) when the fluid is not pumped as a connection is made. During non-drilling activities (tripping pipe, running casing, etc.) the drilling fluid may lie stagnant in the hole for hours or even days. During this period, settling of solids can be especially problematic if the fluid does not have enough structure to support both large and small particulate matter. For these reasons clays, which form associative networks and introduce a yield stress in the fluid, are frequently employed as viscosifiers. They provide both a structural network that suspends solids in low-shear / no-flow situations and are sufficiently shear-thinning to allow pumpability. However, an overly-structured fluid can provide problems as severe as an under-structured fluid. If the fluid builds a sufficiently strong structure, the resultant yield stress required to break the structure (by tripping pipe, initiating pump flow, etc.) and initiate flow will become excessively high. This, in turn, may result in tremendous pressure surges and increases the likelihood of fracturing the formation. The balance between minimizing swab and surge and pump initiation pressures, without allowing barite sag, can be difficult to maintain in fluids that are thixotropic and exhibit a yield stress.

Yield Stress

Yield stress fluids are commonly found in many applications, including foods (mayonnaise), cosmetics, hygiene (shaving creams and toothpaste) as well as those common to the drilling industry (muds and cement). It has long been observed that drilling fluids do not flow unless subjected to a certain load (stress); that is, they are yield stress materials. The yield stress and low-shear-rate viscosity of drilling fluids have become key parameters for hole cleaning, barite sag, and pressure-loss analyses, with the Herschel-Bulkley model becoming the *defacto* standard[1]. It is also well understood that drilling fluids are time-dependant materials; that is, they exhibit thixotropic tendencies, exhibiting a reversible decrease of viscosity of the material in time when a material is made to flow[2,3,4,5]. Yield stress fluids can be defined as fluids that can support their own weight to a certain extent, *i.e.* they can support shear stresses without flowing as opposed to Newtonian fluids. Yield stress behavior and thixotropy are usually considered as separate phenomena, but they show a tendency toward appearing in the same fluid. In addition, they are believed to be caused by the same fundamental physics. The same microstructure present in a fluid that resists large rearrangements (which is responsible for the yield stress), when broken by flow, is believed to be the origin of thixotropy.[5]

The determination of yield stress in a fluid can be accomplished by various means. In the drilling fluids industry, the most common method is through fit of the flow curve measured on a Model 35A-type viscometer to either a Bingham plastic or Herschel Bulkley model. Given well behaved fluids and sufficient data to be used in parameter regression, these methods can result in fairly representative yield stress values. The accuracy of these two models, as well as other prominent models for predicting yield stress, have been called into question.[2] In an effort to better understand

what the "true" value of a fluids yield stress is, the focus of this paper is on experimental methodology and a comparison of the values which may be obtained through differing techniques. The authors also find themselves asking which of the measured values of yield stress are actually relevant to the field performance of a drilling fluid. An explanation of the tests used and their potential utility in the field follows.

Experimental Methodology

Rheological testing was performed on an Anton-Paar MCR301 stress-controlled rheometer (Baker Hughes Drilling Fluids) and an ARES strain-controlled rheometer from TA Instruments (MIT). In general, before testing, all samples were brought to a test temperature of 120°F and then presheared for two minutes at 1022 s^{-1} (600-rpm on a Model 35A viscometer) and the relevant test was run immediately. Multiple test geometries were employed, including profiled parallel plates and a six-vane stirrer to reduce the impact of wall slip on recorded data and evaluate differences in measured yield stress. Large amplitude oscillatory shear (LAOS) tests were performed on a 25-mm plate geometry with a layer of 600 grit sandpaper. The sandpaper was attached to both the top and bottom of the gap, and vacuum grease was then used to seal a 30 mm ring around the bottom sandpaper. During the experiments the gap size was 0.5 mm.

Traditional Yield Stress Analytical Methods

The yield stress, σ_Y, of each fluid was determined through several methods. Initially, the yield stress was determined through *flow curve analysis*. The strain rate was swept from a high rate to a low rate, typically from 1200 s^{-1} to 0.001 s^{-1}, collecting 150 data points over the test region. Several standard models were utilized, along with observation of the yield stress plateau, to determine the yield stress of the fluid. The second method involves an *ascending stress sweep*, performed after preshearing and a rest period for gel formation. Here, the stress is ramped smoothly from a low stress until shear is well developed (>100 s^{-1}) and the strain response of the fluid monitored[6]. The upward inflection point in a strain verses stress curve was taken as the yield stress.

As a third option, the yield stress was also determined experimentally through *sustainable flow tests*.[3,5,7,8] In this test, a series of constant stresses are imposed on the sample, and the viscosity and shear rate are monitored over time. When the applied stress is just above the yield stress of the fluid, viscosity will drop over time, eventually reaching a steady value. When the applied stress is just below the yield stress, the fluid may initially begin to flow, leading to decreasing viscosity; however, over time, the viscosity will increase as flow stagnates. When plotting a series of curves showing the viscosity response over time for different stresses, a bifurcation in the viscosity becomes evident (see Figures 5 and 6). The stress at which this bifurcation occurs is the yield stress of the fluid, below which sustainable flow will not occur.

Finally, a *dynamic yield stress*, σ_{DY}, was also determined through oscillatory testing[6]. For this, either the strain amplitude or stress amplitude was increased at constant frequency, again after preshearing and a rest period for gel formation, until nonlinearity was observed. The stress at deviation from linearity was taken as σ_{DY}.

Superposition Tests

Besides the more traditional methods for evaluating yield stress, by flow curve analysis, ascending stress sweep, sustainable flow, or dynamic analysis, two non-traditional approaches were taken. The first of these is superposition of a steady stress and oscillatory flows. Oscillatory testing of fluids best characterizes the structural behavior of fluids under static (no-flow) conditions. Through superposition of an oscillatory test within the linear viscoelastic region on a steady stress, changes in viscoelastic properties can be monitored near the yield stress and when the fluid is actively flowing.

Despite periodic study over the past four decades, the viscoelastic properties of fluids under shear has received relatively little attention. Fluids can present some unusual behavior in such tests, including exhibiting a phase angle of greater than 90° and negative storage modulus at low frequencies. These phenomenon have been predicted by models and were experimentally observed by several authors.[9,10,11,12,13] Potential for misinterpretation of data from such tests exists, as no commercial instruments allow for a negative storage modulus.

For superposition tests, a constant stress was applied up to the measured yield stress of a sample, similar to the previously detailed procedures[13]. Oscillations were performed in parallel to the imposed stress, at constant stress amplitudes below the measured dynamic yield stress (and thus in the linear viscoelastic region when no superposed stress was present). Either an oscillatory frequency sweep, from 100-rad/sec to 0.1-rad/sec, or an oscillatory time sweep, at 0.81-rad/sec for two hours, were employed. Because tests were performed with the shear and oscillation in parallel, a coupling of the flows results and the viscoelastic moduli no longer retain the same physical interpretation as in linear viscoelastic tests. Observations were made as to when an imposed stress resulted in coupling / nonlinearity in the viscoelastic moduli, G' and G''. This "break stress", where transitory flow is induced and the fluid no longer behaves in a purely linear, uncoupled manor, is of interest when considering the yield stress of fluids. As the coupling of flows results in structural breakdown in the fluid, even under low perturbation, this break stress is of potential interest when considering drilling fluids, which rely on structure to suspend solids in the fluid.

LAOS Motivation and Description

The most common method to characterize nonlinear rheological properties of complex fluids is a steady-state non-Newtonian viscosity measurement, $h(\dot{g})$. In many applications, and in particular with oilfield drilling muds, the fluid flow will start and stop over numerous timescales, and

the time dependent properties of the fluid may become significant. Researchers have addressed the issue of characterizing time-dependent viscous properties by utilizing thixotropic loop tests. These tests are performed by ramping shear-rate up to a particular value over a specified time, and subsequently ramping shear-rate back down. Time dependent properties are indicated by hysteresis (i.e. loops) in the resulting viscosity curves. Thixotropic loop tests successfully indicate time dependency, but only capture viscous properties, leaving no room for the (time dependent) elastic nature of the material to be characterized.

Large amplitude oscillatory shear (LAOS) is a test method which systematically connects steady flow viscosity $h(\dot{g})$, linear viscoelastic moduli G'(ω) and G''(ω), and nonlinear viscoelastic properties[14], allowing for nonlinear viscous, elastic, and thixotropic effects to be characterized simultaneously. This systematic technique thus provides a full "rheological fingerprint" of a complex fluid. In strain-controlled LAOS flow, the imposed strain takes the form $g(t) = g_0 \sin wt$, which consequently imposes a phase-shifted strain-rate $\dot{g}(t) = g_0 w \cos wt$. Steady flow is recovered in the limit of small frequency, $w \to 0$, whereas linear viscoelasticity is recovered in the limit of small strain amplitude, $g_0 \to 0$. For small and finite ω, when viscous effects dominate, a thixotropic loop test is recovered since the shear-rate ramps up and down sinusoidally.

The two-parameter input of LAOS tests, {ω,γ_0}, defines an operating space known as a Pipkin diagram[15]. Displaying various LAOS results via the Pipkin diagram represents different rheological fingerprints of a material response. Each imposed value of {ω,γ_0} represents a unique oscillatory test with corresponding oscillatory signals of stress, strain, and strain-rate, along with calculated material parameters such as viscoelastic moduli.

The oscillatory stress, strain, and strain-rate signals are readily visualized by the use of Lissajous curves. Elastic Lissajous curves are parametric plots of stress σ(t) vs. strain γ(t), whereas viscous Lissajous curves are parametric plots of stress σ(t) vs. strain-rate $\dot{g}(t)$. A purely elastic material response appears as a line on the elastic Lissajous curve of σ(t) vs. γ(t). A loop is formed here if viscous dissipation is present. Lissajous curves appear as ellipses in the linear viscoelastic regime, owing to the stress response being a single-harmonic function.

A nonlinear viscoelastic response, such as a yield stress, will distort the elliptical shape. To illustrate the Lissajous curve features associated with yield stress fluids, we consider the LAOS response of three idealized models: Perfectly Plastic, Bingham Plastic, and Bingham Elasto-Plastic. The Perfectly Plastic model has no elasticity before yield, and imposed flow results in a constant flow stress. The constitutive equation of the Perfectly Plastic model is given by

$$s = s_Y \operatorname{sgn}(\dot{g})$$

where σ_Y is the yield stress, $\dot{g}$ is the shear-rate, and sgn(x) is the sign function which is -1, 0, or +1 when x is negative, zero, or positive, respectively. The second model we consider is the Bingham Plastic, which also has no elasticity before yield. After yield, however, the flow stress increases linearly with the shear-rate. The constitutive equation for the Bingham Plastic model, written in terms of imposed deformation, is

$$s = s_Y \operatorname{sgn}(\dot{g}) + m_{Bn}\dot{g}_0\left(\frac{\dot{g}}{\dot{g}_0}\right)$$

where μ_{Bn} is the Bingham plastic viscosity, and the equation has been written specifically for LAOS flow with shear-rate amplitude $\dot{g}_0 = g_0 w$. The non-dimensional Bingham number, Bn* characterizes the model parameters in LAOS flow, $Bn^* = s_Y / m_{Bn}\dot{g}_0$.

The third yield stress model considered is the Bingham Elasto-Plastic. This model responds as a linear elastic solid prior to yield, with shear modulus G. After yield, the material flows as a Bingham Plastic with stress linearly proportional to shear-rate. When the flow stops, $\dot{g} = 0$, a residual stress σ_Y remains, which corresponds to a recoverable elastic strain, σ_Y/G, which was accumulated prior to yield. In LAOS, the flow changes direction when shear-rate is instantaneously zero, $\dot{g} = 0$. At this point the recoverable elastic strain is first eliminated to bring σ = 0, after which elastic deformation continues until yield. The constitutive equation for the Bingham Elasto-Plastic model, written specifically for LAOS flow, is given by

$$\frac{s}{s_Y} = \begin{cases} \operatorname{sgn}(-\dot{g}) + \dfrac{Gg_0}{s_Y}\left(\dfrac{g^*}{g_0}\right) & \left|g^*\right| < 2\dfrac{s_Y}{G} \\ \operatorname{sgn}(\dot{g}) + \dfrac{m_{Bn}\dot{g}_0}{s_Y}\left(\dfrac{\dot{g}}{\dot{g}_0}\right) & \left|g^*\right| > 2\dfrac{s_Y}{G} \end{cases}$$

where γ* is the strain that has accumulated since the shear-rate was instantaneously zero. The model's response to LAOS flow is governed by two non-dimensional parameters, the LAOS Bingham number $Bn^* = s_Y / m_{Bn}\dot{g}_0$, and the normalized yield strain γ_y/γ_0, where $\gamma_y = \sigma_y/G$.

The LAOS response of each model is given in Figure 1. The most prominent feature of these yield stress models is a nearly rectangular elastic Lissajous curve. The Perfectly Plastic model has vertical sides and a flat top and bottom. The Bingham Plastic model also has vertical sides, but is rounded on the top and bottom because flow stress is proportional to shear-rate. The Bingham Elasto-Plastic adds an additional feature, sloped sides, which are caused by the elasticity for stresses below the yield stress. The *viscous* Lissajous curves in Figure 1 have correspondingly distinct features. The plastic viscosity, μ_{Bn}, of each model is indicated by the linear portions of the curves in the upper-right and lower-left. Pre-yield elasticity is indicated by the enclosed area in the center of the

viscous Lissajous curve of the Bingham Elasto-Plastic response.

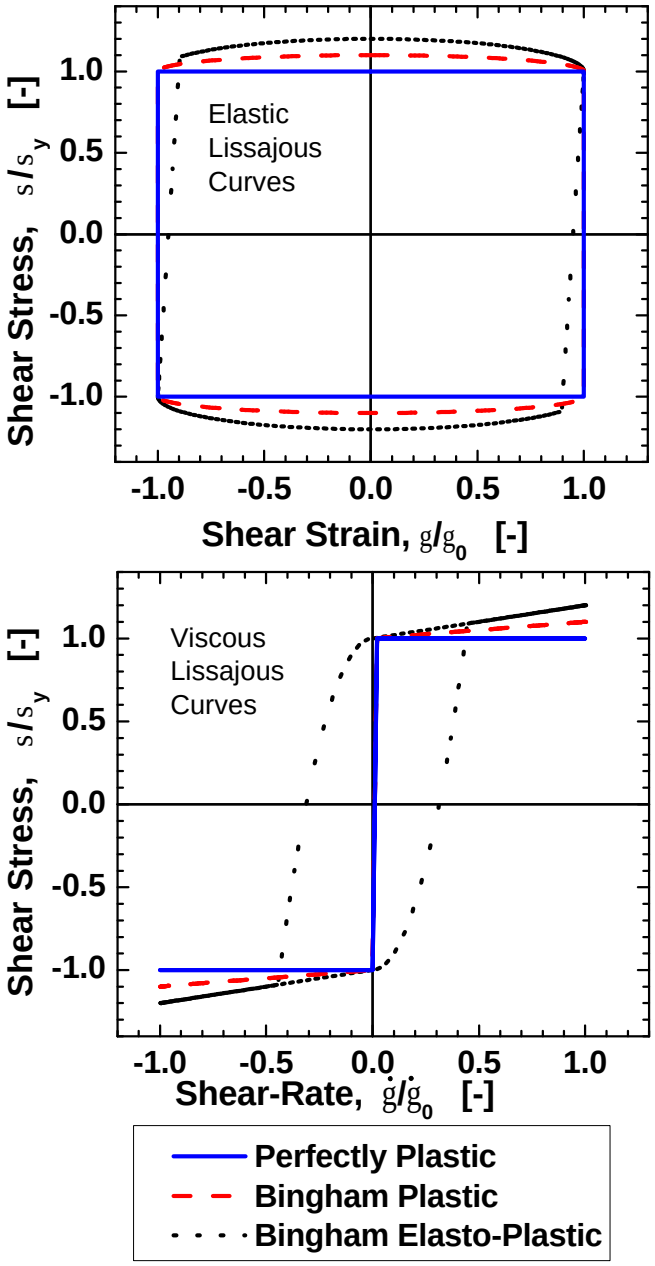

Figure 1 LAOS response of three idealized yield stress models: Perfectly Plastic, Bingham Plastic (Bn*=10), and Bingham Elasto-Plastic (Bn*=5, γ_y/γ_0=0.05). Lissajous curves are shown to illustrate the typical features of yield stress fluids in LAOS flow.

An additional analysis may be applied to the LAOS response; the total stress may be decomposed into its elastic and viscous contributions[16]. The resulting elastic stress is only a function of strain, $s'(g)$, and the viscous stress component only a function of strain-rate, $s''(\dot{g})$. These elastic and viscous stresses, $s'(g)$ and $s''(\dot{g})$, can be displayed on the elastic and viscous Lissajous curves, respectively, which results in single-valued lines, rather than loops. In the linear viscoelastic regime these decomposed stresses appear as lines of constant slope. In the nonlinear regime (large g_0) the elliptical shapes of the Lissajous curves (and the constant slopes of the decomposed stresses) are distorted. The distortion of Lissajous curves can be quantified and physically interpreted using a recent framework presented by Ewoldt *et al.*[17]

Test Fluids

A number of fluids were examined in the process of this research. The results presented here cover seven fluids. Two fluids were laboratory mixed water-based muds (WBM1 and WBM2). WBM1 is a 10-lb/gal, lignosulfonate fluid in 10% sodium chloride, is viscosified with 20-lb/bbl of bentonite, and includes modified starch for fluid loss control. WBM2 is a 16-lb/gal, fresh-water clay/polymer fluid with 20-lb/bbl of bentonite and a modified starch. Two fluids were laboratory mixed oil-based muds (LOBM1 and LOBM2). LOBM1 is a 14-lb/gal, 80/20 oil/water ratio mud viscosified with 5-lb/bbl organophilic clay and an organic rheological modifier. LOBM2 is a 13-lb/gal, 80/20 oil/water ratio mud viscosified with 5-lb/bbl organophilic clay. None of the laboratory-mixed fluids included simulated drilled solids.

The final three fluids were samples of oil-based muds obtained from field operations (FOBM1, FOBM2, and FOBM3). All three contained reasonable amounts of low-gravity solids (4% - 6%) incorporated in the fluid during drilling. FOBM 1 and FOBM3 have roughly the same formulation as LOBM1, with the exception that FOBM3 has an added filtration control material. FOBM2 is a 13-lb/gal 80/20 oil/water ratio mud with an undetermined amount of organophilic clay.

Flow Curve Analysis

Flow curves presenting the rate-dependence of stress and viscosity were generated for each of the seven fluids. Experiments were conducted either as a controlled rate sweep or controlled stress sweep and included a range of rates from less than 0.001 s^{-1} to greater than 1000 s^{-1}. The resultant curves are presented in Figures 2 and 3. The seven fluids have, in general, comparable viscosity profiles. WBM2 exhibits the greatest viscosity throughout the test region, and is significantly higher than any other fluid tested. While WBM1 exhibits the lowest viscosity at high rates, LOBM2 has the lowest viscosity at low strain rates. FOBM2 shows a significantly higher viscosity at high rates than any fluid (with the exception of WBM2) but shear-thins less than, and has a low-rate viscosity comparable to, the other fluids. Little else can be observed from the viscosity profile of these fluids.

More interesting conclusions can be drawn from examination of the stress profile of these fluids. The first point of interest is that few of these fluids actually demonstrate a clean, well-defined yield stress plateau. WBM2

and FOBM1 both exhibit a definite yield plateau, with WBM2 additionally exhibiting an inflection in the stress curve at very

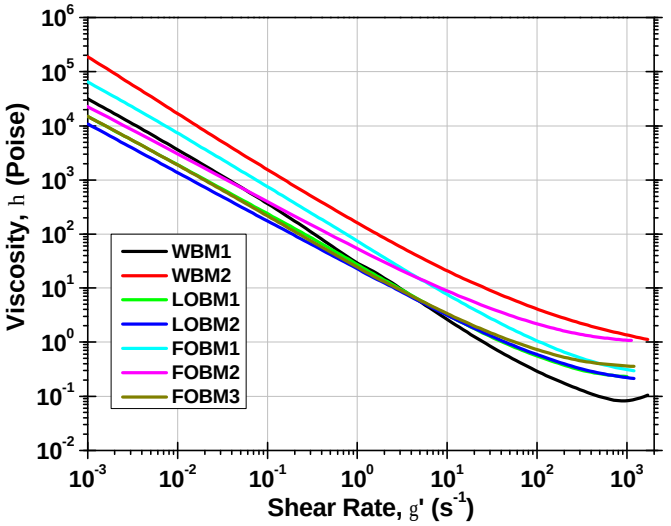

Figure 2 Flow curve of viscosity as a function of strain rate for the test fluids. All tests were conducted at 120°F after pre-shearing the fluid for two minutes.

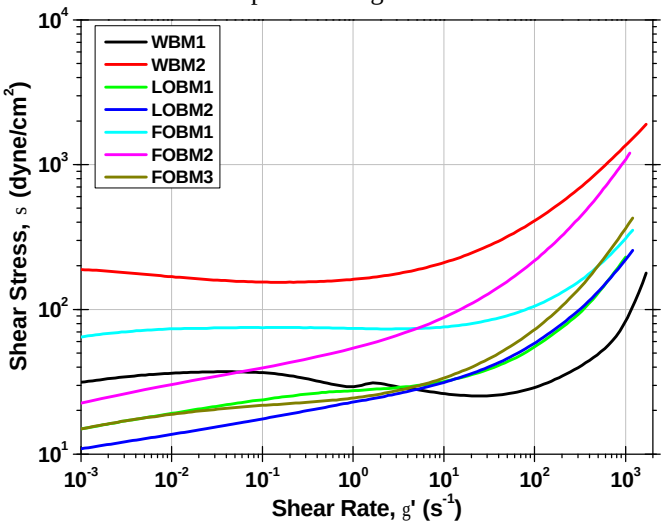

Figure 3 Flow curve of stress as a function of strain rate for the test fluids. All tests were conducted at 120°F after pre-shearing the fluid for two minutes.

low rates. This is due to structuring of the fluid during flow in the vein of the predictions of Møller, Mewis, and Bonn[5]. By comparison, FOBM1 demonstrates slight shear-thinning at very low rates, below the region of the yield stress plateau. WBM1 demonstrates a mix of these two behaviors, and exhibits something of an unclear yield plateau. The other four fluids, the two laboratory oil-based muds and two of the field oil-based muds, do not exhibit any yield plateau. Such behavior could be expected for the laboratory mixed fluids, as they did not contain any sort of drilled solids and have not experienced the shear and aging that work to swell the clays and form a thixotropic, yielding fluid. However, the reasoning for the lacking yield plateau in the field muds – even when measurements are conducted to 10^{-5} s^{-1} (see Figure 4) – is as yet unknown.

One consequence of the lack of a well-established yield plateau in the drilling fluids is poor fitting of standard yield stress models. The effectiveness of the Bingham plastic and Herschel-Bulkley models, which are widely used in the drilling fluids industry, and the more recent Mendes-Dutra model[18], are compared to FOBM1 and FOBM2 in Figure 4. Additionally, the predicted yield stress for all seven fluids from these three models is presented in Table 1.

For the case of FOBM1, all three models fit the experimental data reasonably well and the yield stresses predicted by the three are very similar (see Table 1). The Mendes-Dutra model fits better the shear-thinning exhibited at very low rates; however, if such low rate data is not available (as is usually true in the field) then either the Bingham plastic or Herschel-Bulkley models would provide excellent modeling of the fluid. With FOBM2, however, the three models predict significantly different yield stresses. Additionally, outside of the high-rate shear thinning region, none of the three model the flow behavior well. Any predictions made on this fluid from these standard models would be flawed. FOBM2 has been observed to be highly thixotropic, however, and some yield behavior is to be expected. The question remains as to how such a fluid should be treated in terms of yielding and flow.

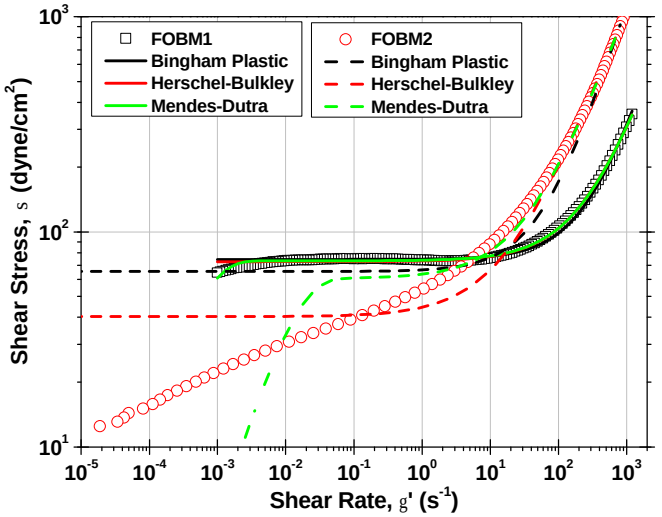

Figure 4 Modeling the flow curves of FOBM1 and FOBM2. The fluids were modeled using the Bingham plastic, Herschel-Bulkley, and Mendes-Dutra models.

When examining the model predictions for yield stress of the other fluids, a similar result as found with FOBM2 is observed. For WBM2, which like FOBM1 exhibited a clear yield stress plateau, the results of the three models are again comparable. With WBM1, which exhibits a more variable yield plateau, the model predictions are also comparable to

each other. However, for the four fluids which continue to shear thin and do not exhibit a yield plateau, the predictions of the models show somewhat less agreement. As with FOBM2, the models weight prediction on the high strain rate region; the modeled yield stress becomes based not on any apparent plateau in the curve but on where the mathematical inflection in a best-fit curve occurs. In such cases, which only become apparent when tests are conducted below the strain rate range of standard Model 35A viscometers, speaking of a yield stress in the fluid becomes meaningless and the fluid must be considered outside the traditional frame in which drilling fluids have been placed.

Table 1 Modeled yield stress (in dyne/cm^2) for the seven test fluids from the Bingham plastic, Herschel-Bulkley, and Mendes-Dutra models.

s_Y (dyne/cm^2)	Bingham plastic	Herschel-Bulkley	Mendes-Dutra
WBM1	29.9	30.7	26.2
WBM2	171.7	161	162.8
LOBM1	21.9	14.3	18
LOBM2	16.1	12.6	19.8
FOBM1	73.4	72.5	73.4
FOBM2	65.6	40.3	60.5
FOBM3	20.8	18.9	23.5

Ascending Stress and Sustainable Flow Tests

Besides model fitting to predict yield stress, several experimental approaches were taken to measure the yield stress. Two of these, ascending stress sweeps and sustainable flow tests, involved rotational testing of the fluids under controlled stresses. Results of these are presented in Table 2. For ascending stress sweeps, the samples were initially sheared at 1022 s^{-1} for two minutes and then allowed a rest period of 10-seconds, 10-minutes, or 30-minutes for formation of a gel structure before the stress sweep was performed. For sustainable flow tests, a series of constant stresses were imposed on the sample after preshearing. Data was collected over one hour for each constant stress test. Through observation of the viscosity over time, the stress at which the viscosity profiles began to bifurcate – either moving toward stagnation or very low constant flow – was observed and recorded as the observed yield stress. Examples of these curves can be seen in Figures 5 and 6.

The viscosity bifurcation is very clear in Figure 6, for FOBM3. As can be observed, a change in the applied stress from 30- to 32.5-dyne/cm^2 results is a dramatic difference in the long-time (>30 seconds) viscosity of the fluid. With an additional increase in stress from 32.5- to 35-dyne/cm^2 another small change in observed; at very long times (approaching 1 hour of testing) the viscosity for an imposed 35-dyne/cm^2 stress is observed to plateau while the 32.5-dyne/cm^2 stress continues to show increasing viscosity. A less dramatic but equally distinct bifurcation in viscosity is observed from FOBM2 (Figure 5), occurring between 30- and 40-dyne/cm^2.

The observed sustainable flow yield stress for FOBM3 (35-dyne/cm^2) is lower than the yield stresses measured from ascending stress sweeps, but greater than those predicted from the three models. For LOBM2 and FOBM2, the sustainable flow yield stress is significantly lower than those found from modeling or ascending stress sweeps. In general, the model predictions were similar to the yield stresses measured by ascending stress sweeps.

Table 2 Measured yield stress (in dyne/cm^2) for the seven test fluids as observed from ascending stress sweeps and sustainable flow tests. All tests were performed at 120°F using profiled parallel plates.

s_Y (dyne/cm^2)	Ascending Stress Sweep			Sustainable Flow Test
	10-sec. gel	10-min. gel	30-min. gel	
WBM1	10.4	26.8	40.3	--
WBM2	208.6	249.6	473.1	--
LOBM1	42.1	49.2	50.4	--
LOBM2	22.6	23.2	--	1
FOBM1	38.3	66.7	78.4	95
FOBM2	60.2	68.6	67.6	38
FOBM3	39.5	42.4	46.1	35

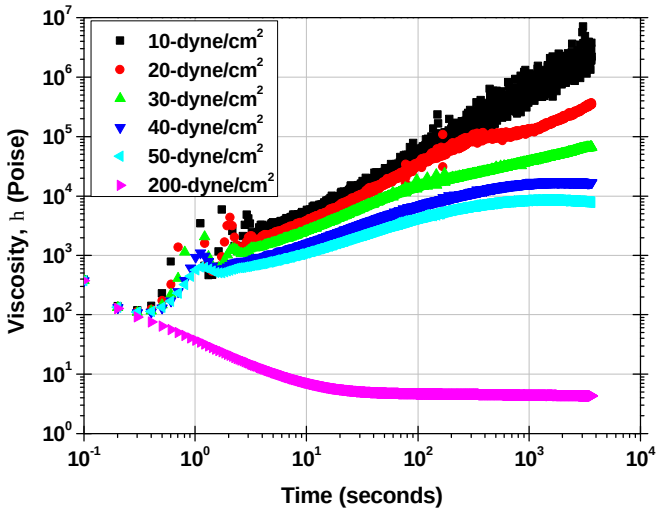

Figure 5 Constant stress curves from sustainable flow tests for FOBM2 at 120°F. The bifurcation of the viscosity curves between induced stresses of 30- and 40-dyne/cm^2 is readily apparent.

Some work was also done to compare the measurements made by different geometries. The results for FOBM3 for these tests are presented in Table 3. This compares the results of ascending rate sweeps using profiled parallel plates, a double gap couette, and a six-vane paddle-type stirrer. With the exception of the tests performed after a 10-second rest

period with the stirrer, very little difference is observed in the measured yield stresses.

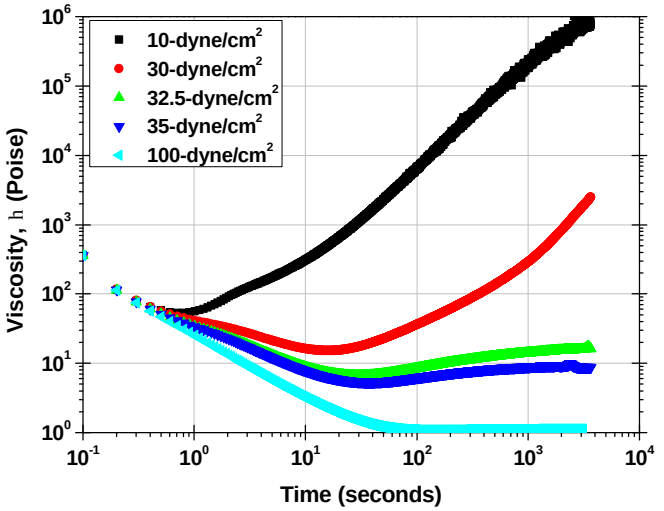

Figure 6 Constant stress curves from sustainable flow tests for FOBM3 at 120°F. The bifurcation of the viscosity curves between induced stresses of 30- and 32.5-dyne/cm^2 is readily apparent.

Table 3 Comparison of measured yield stress (in dyne/cm^2) for FOBM3 from ascending stress sweeps. Tests were performed at 120°F using profiled parallel plates, a double gap couette, or 6-vane stirrer.

s_Y (dyne/cm^2)	Profiled Plates	6-Vane Stirrer	Double Gap Couette
10-sec. gel	39.5	28	39.5
10-min. gel	42.4	39	42.4
30-min. gel	46.1	45.9	46.1

Dynamic Yield Stress

In all, from flow curve modeling, ascending stress sweeps, and sustainable flow tests, no clear picture has been presented for what could be considered the yield stress of these fluids. For WBM2 and FOBM1, more agreement has been found; however, when considering the other fluids we must begin to ask which of these measurements is most relevant to drilling fluids, especially when considering more than the hydraulic implications of the fluid. For this reason, we begin to examine other, less commonly used, methods for evaluating yield in fluids.

Oscillatory strain and stress amplitude sweeps were preformed on the test fluids and the dynamic yield stress, σ_{DY}, was determined at the point when nonlinearity was observed in the storage modulus. The results of these tests are presented in Figure 7. As would be expected, these values differ significantly from the previously measured yield stresses for the samples (see Tables 1 and 2). This is because the dynamic yield test, by definition, identifies the point at which the response of the fluid becomes nonlinear, though inception of flow in may not have occurred. It is observed that there is a significant difference between the measured dynamic yield stresses for LOBM1, LOBM2, and FOBM3 – which are all relatively low – and those measured for WBM2, FOBM1, and FOBM2 – all of which are relatively high. This observation becomes more interesting when it is considered that LOBM1 and LOBM2 have both been observed to experience dynamic barite sag; whereas WBM2, FOBM1, and FOBM2 have not exhibited sag. This distinction provides a potentially interesting method for indirect rheological evaluation of dynamic sag.

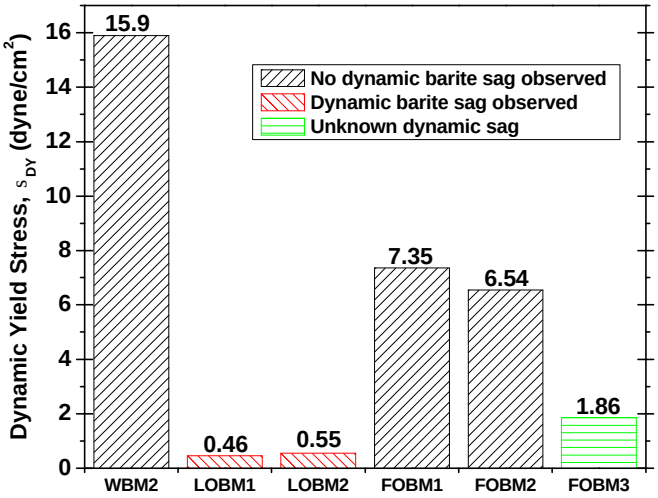

Figure 7 Comparison of the dynamic yield stress, σ_{DY}, for the test fluids. All tests were conducted at 120°F using profiled parallel plates. Fluids which were observed to dynamically sag are in red, while those with no dynamic sag are in black. No observations were made for FOBM3.

Superposition Break Stress

Superposition tests were performed as previously described by Maxey[13]. Tests were conducted at a constant stress amplitude, σ_a, which was selected to be below the dynamic yield stress of the fluids (and thus within the linear viscoelastic region). Results from such tests are presented in Figures 8 and 9.

In Figure 8, the superposition of an oscillatory frequency sweep (from 100-rad/sec to 0.1-rad/sec) on a series of constant stresses is observed. It can be seen that imposed stresses of up to ~20-dyne/cm^2 result in nominal deviation from the baseline measurements of G', the storage modulus, and δ, the phase angle, taken with superposed constant stress. However, above 20-dyne/cm^2, some nonlinearity or coupling of the rotational and oscillatory measurements is observed as flow is initiated in the sample. Thus, a break stress of between 20 – 22 dyne/cm^2 is measured for this sample. This value is of potential interest as it applies to the complex flow occurring in an annulus, where the bulk of the fluid experiences very little

shear but perturbations may be present in sufficient degree to disturb the gel structure forming in the mud.

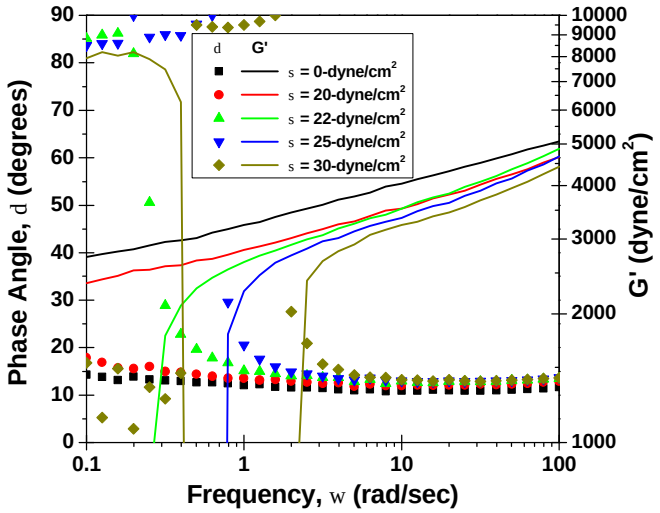

Figure 8 Superposed constant stress and oscillatory frequency sweeps at 120°F and σ_a=7-dyne/cm^2 for FOBM1. Apparent nonlinearity / coupling of flow and oscillations is observed to occur at between 20-22 dyne/cm^2.

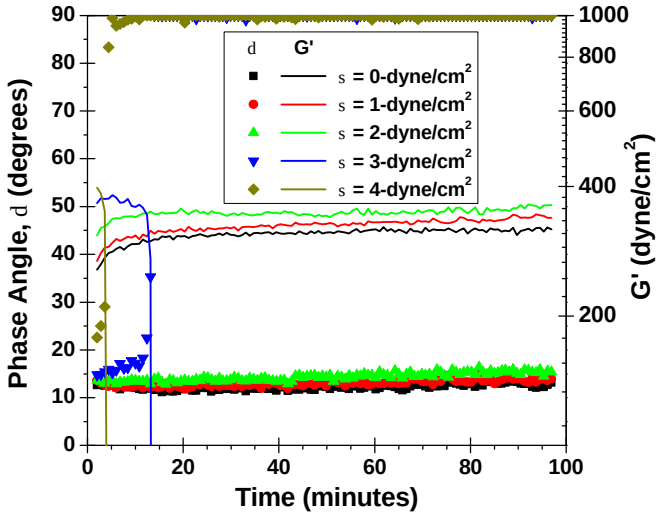

Figure 9 Superposed constant stress and oscillatory time sweep at120°F, 0.81-rad/sec, and σ_a =0.5-dyne/cm2 for LOBM2. Apparent nonlinearity / coupling of flow and oscillations is observed to occur at between 2-3 dyne/cm^2.

The superposition results for LOBM2, seen in Figure 9, present an oscillatory time sweep (at 0.81-rad/sec) on a series of constant stresses. Similar to the superposed frequency sweep in Figure 8, the onset of nonlinearity / coupling between rotational and oscillatory flows is readily observed. For LOBM2, the break stress due to flow coupling is observed at between 2-3 dyne/cm^2, an order of magnitude lower than that observed for FOBM1. This difference echoes the significant disparity between the measured sustainable flow yield stresses and dynamic yield stresses for the two fluids. Again, this value becomes of greater interest when considering that LOBM2 has been observed to exhibit dynamic barite sag while FOBM1 has not.

LAOS Results and Discussion

As a final test methodology, strain-controlled large amplitude oscillatory shear (LAOS) was used to examine the yielding behavior of drilling fluid FOBM1. Here we focus on the raw oscillatory data associated with the LAOS tests, presented in the form of Lissajous curves (Figure 10). None of the curves in Figure 10 is elliptical, which indicates that all of the viscoelastic responses are nonlinear. The dynamic yield stress, s_{DY}, is defined as the initial deviation from a linear oscillatory response. From this data set (Figure 10) it can be stated that the dynamic yield stress is $s_{DY} < 56.6$ dyne/cm^2, as indicated by the minimum observed stress at $\{w = 0.15, g_0 = 1\}$. Although this result is consistent with the stress-controlled results of Figure 7 ($s_{DY} = 7.35$ dyne/cm^2), lower imposed strain amplitudes are necessary to access the linear regime and give a clear value for s_{DY} under strain-controlled oscillations.

The Lissajous curves of Figure 10 can be compared with the responses of idealized yield stress models (Figure 1) to evaluate viscous, elastic, and thixotropic characteristics. It is observed that the elastic Lissajous curves at $\{w = 0.15, g_0 = 10\}$ and $\{w = 0.75, g_0 = 10\}$ most closely resemble the idealized yield stress model behavior of Figure 1. From visual inspection, the Bingham Elasto-Plastic model is the best choice to represent the response of FOBM1 at these low frequencies and large strain amplitudes. The elastic Lissajous curve at $\{w = 0.15, g_0 = 10\}$ demonstrates elasticity below the yield stress (indicated by the sloped sides of the curve), and a plastic yielding indicated by the corners of the curve which give a square rather than rounded shape. Complementary features on the viscous Lissajous curve in Figure 10b indicate these same elasto-plastic characteristics at low frequency and large strain-amplitude. The yield stress indicated by these elasto-plastic curves is approximately 100 dyne/cm^2. This *completely yielded* critical stress is similar to the yield stress measured with the sustainable flow methodology.

None of the idealized yield stress models of Figure 1 qualitatively describe the responses at lower strain-amplitudes, because here the fluid is not fully yielded. This partially yielded state is indicated by significant elasticity which remains during flow, as evidenced by the sloped top and bottom edges of the elastic Lissajous curves (e.g. for $g_0 = 1$). Furthermore, a fully yielded plastic response is absent at the largest imposed frequency, $w = 18.75$ rad/s. This response at high frequency appears to be viscoelastic, rather than elasto-plastic, since the resulting elastic Lissajous curve is devoid of sharp corners and appears as a round shape. This can be

interpreted in terms of the experimental timescale ($1/w = 0.053$ seconds) being shorter than the thixotropic restructuring time, which prevents the formation of a yield stress at these sufficiently large oscillatory frequencies.

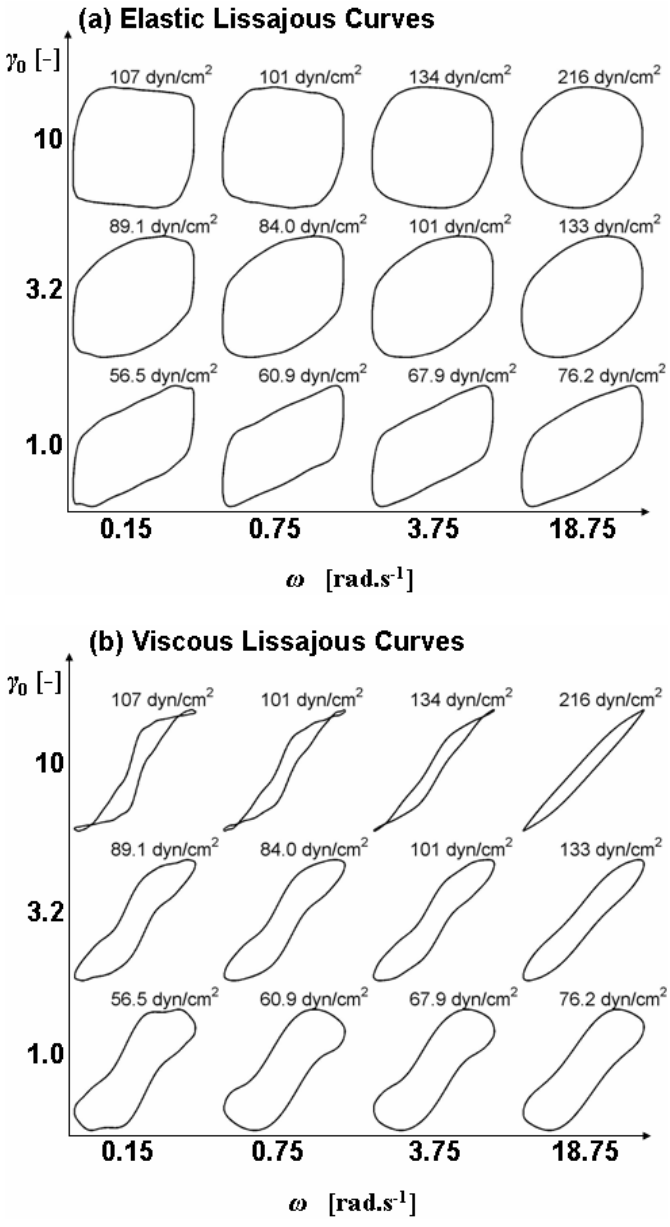

Figure 10 Experimental data from 12 oscillatory shear tests with FOBM1. Individual orbits are positioned according to the imposed $\{?,?_0\}$; (a) Elastic Lissajous curves of stress s/s_{max} vs. strain g/g_0, (b) Viscous Lissajous curves of stress s/s_{max} vs. strain-rate $\dot{g}/\dot{g}_0$. The maximum stress, s_{max}, is indicated above each curve. For low frequencies and large strain amplitudes the material behaves similarly to the elasto-plastic yield stress model.

These results demonstrate that Lissajous curves from LAOS tests are a sensitive indicator of the appropriateness of yield stress models under various operating regimes of amplitude and cyclic frequency. The Pipkin diagram of Figure 10 indicates the operating regime where more traditional yield stress models may suffice (low frequency and large amplitude) and also where complex elastic and thixotropic effects are significant. Elasticity is not accounted for in the models traditionally used in the drilling industry, and LAOS can indicate when the assumption of negligible elasticity is inappropriate.

Conclusions

- Drilling fluids have been treated as yield stress materials; however, evidence has pointed to cases where drilling fluids do not act as traditional yield stress materials. This requires further rheological characterization of the fluid, beginning with expanded flow curves to strain rates below 0.1 s^{-1}, and potentially different modeling for better hydraulic predictions.
- Multiple methods exist for the measurement of yield stress. Some variability is found between methods, and between measured yield stress and model predictions. This is complicated by the lack of an apparent yield plateau in some fluids. Care should be taken to evaluate which method is most appropriate for a particular drilling fluid. Additionally, when tests are performed with care, no difference is observed in the results found using various test geometries.
- Non-traditional methods for measurement of a yield stress have been studied. Some of these hold particular interest in evaluation of the potential of a fluid for dynamic barite sag. Differentiation in the measured dynamic yield stress or break stress from superposition of shear and oscillations could provide a measure for classification of potential for sag in the fluid.
- The yield stress found at low frequency, high strain in LAOS tests is similar to the yield stress from sustainable flow measurements.
- Multiple complex behaviors are observed in the drilling fluid through LAOS testing. At low strains and frequencies, elasticity is evident in the fluid, while at higher strains and low frequency, the fluid is observed to act in a nearly pure plastic manor. At high frequencies, above the characteristic timescale for thixotropic restructuring in the fluid, the fluid is more viscoelastic in nature (where most attention has been given to drilling fluid discussion).

Nomenclature

LAOS	*= Large amplitude oscillatory shear*
s	*= stress (dyne/cm^2)*
s_a	*= stress amplitude (dyne/cm^2)*
s_Y	*= yield stress (dyne/cm^2)*
s_{DY}	*= dynamic yield stress (dyne/cm^2)*
h	*= viscosity (Poise)*
w	*= angular frequency (rad/sec)*
g	*= strain*
G'	*= storage modulus (dyne/cm^2)*
G''	*= loss modulus (dyne/cm^2)*
d	*= phase angle*

References

1. Zamora, M. and D. Power, "Making a Case for AADE Hydraulics and the Unified Rheological Model," AADE 2002 Drilling Fluids Conference, (AADE-02-DFWM-HO-13).
2. Maxey, J., "Thixotropy and Yield Stress Behavior in Drilling Fluids", AADE 2007 Drilling Fluids Conference, (AADE-07-NTCE-37).
3. Coussot, P., Q.D. Nguyen, H.T. Huynh, and D. Bonn, "Viscosity bifurcation in thixotropic, yielding fluids," *J. Rheo.* v. 46 (2002), 573-589.
4. Jachnik, Richard: "Drilling Fluid Thixotropy and Relevance," *Ann. Trans. Nordic Rheo. Society*, v. 13 (2005).
5. Møller, Peder C.F., Jan Mewis, and Daniel Bonn: "Yield Stress and thixotropy: on the difficulty of measuring yield stress in practice," *Soft Matter* v. 2 (2006), 274-283.
6. Chen, T., "Rheological Techniques for Yield Stress Analysis," TA Instruments Applications Note, AAN017.
7. Herzhaft, B, A. Ragouillaux, and P. Coussot, "How To Unify Low Shear-Rate Rheology and Gel Properties of Drilling Muds: A Transient Rheological and Structural Model for Complex Well Applications," 2006 IADC/SPE Drilling Conference (IADC/SPE 99080).
8. Ragouilliaux, A., F. Bertrand, and P. Coussot, "Flow instability and shear localization in a drilling mud," *Rheo. Acta* v. 46 (2006), 261-271.
9. Jones, T.E., and Walters, K., "The behavior of materials under combined steady and oscillatory shear", *J. Phys. A*, v. 4 (1971), pp. 85-100.
10. Powell, R.L., and Schwarz, W.H., "Nonlinear Dynamic Viscoelasticity", *J. Rheo.*, v. 23 (1979), pp. 323-352.
11. Mewis, J., Kaffashi, B., Vermant, J., and Butera, R.J., "Determining Relaxation Modes in Flowing Associative Polymers Using Superposition Flows", *Macromolecules*, v. 34 (2001), pp. 1376-1383.
12. Anderson, V.J., Pearson, J.R.A., and Sherwood, J.D., "Oscillation superimposed on steady shearing: Measurements and predictions for wormlike micellar solutions", *J. Rheo.*, v. 50 (2006), pp. 771-796.
13. Maxey, Jason: "Rheological Analysis of Static and Dynamic Sag in Drilling Fluids," *Ann. Trans. Nordic Rheo. Society*, v. 15 (2007).
14. Dealy, J. M. and K. F. Wissbrun, *Melt rheology and its role in plastics processing: theory and applications* (Van Nostrand Reinhold, New York, 1990).
15. Pipkin, A. C., *Lectures on viscoelasticity theory* (Springer-Verlag, New York, 1972).
16. Cho, K. S., K. H. Ahn and S. J. Lee, "A geometrical interpretation of large amplitude oscillatory shear response," *J. Rheo.*, v. 49 (2005), 747-758.
17. Ewoldt, R. H., G. H. McKinley and A. E. Hosoi, "Fingerprinting Soft Materials: A Framework for Characterizing Nonlinear Viscoelasticity," arXiv 0710.5509v1, [cond-mat.soft] (2007)
18. Mendes, Paulo R. Souza and Eduardo S. S. Dutra: "A Viscosity Function for Viscoplastic Liquids," *An. Trans. Nordic Rheo. Soc.*, v. 12 (2004), 183-188.